British Journal of Pharmacology (2004) 143, 411–421
www.nature.com/bjp

Characterization of the human HCN1 channel and its inhibition by capsazepine

[1]Catherine H. Gill, [1]Andrew Randall, [2]Stewart A. Bates, [1]Kerstin Hill, [1]Davina Owen, [3]Phil M. Larkman, [4]William Cairns, [4]Shahnaz P. Yusaf, [2]Paul R. Murdock, [1]Paul J.L.M. Strijbos, [4]Andrew J. Powell, [1]Christopher D. Benham & *,[5]Ceri H. Davies

[1]Neurology & GI CEDD, GlaxoSmithKline, New Frontiers Science Park North, Third Avenue, Harlow, Essex CM19 5AW; [2]Genetics Research, GlaxoSmithKline, New Frontiers Science Park North, Third Avenue, Harlow, Essex CM19 5AW; [3]Department of Pharmacology, University of Edinburgh, 1 George Square, Edinburgh EH8 9JZ; [4]Discovery Research Biology, GlaxoSmithKline, New Frontiers Science Park North, Third Avenue, Harlow, Essex CM19 5AW and [5]Psychiatry CEDD, GlaxoSmithKline, New Frontiers Science Park North, Third Avenue, Harlow, Essex CM19 5AW

1 The human hyperpolarization-activated cyclic nucleotide-gated 1 (hHCN1) subunit was heterologously expressed in mammalian cell lines (CV-1 and CHO) and its properties investigated using whole-cell patch-clamp recordings. Activation of this recombinant channel, by membrane hyperpolarization, generated a slowly activating, noninactivating inward current.

2 The pharmacological properties of hHCN1-mediated currents resembled those of native hyperpolarization-activated currents (I_h), that is, blockade by Cs^+ (99% at 5 mM), ZD 7288 (98% at 100 μM) and zatebradine (92% at 10 μM). Inhibition of the hHCN1-mediated current by ZD 7288 was apparently independent of prior channel activation (i.e. non-use-dependent), whereas that induced by zatebradine was use-dependent.

3 The VR1 receptor antagonist capsazepine inhibited hHCN1-mediated currents in a concentration-dependent ($IC_{50} = 8\ \mu$M), reversible and apparently non-use-dependent manner.

4 This inhibitory effect of capsazepine was voltage-independent and associated with a leftward shift in the hHCN1 activation curve as well as a dramatic slowing of the kinetics of current activation.

5 Elevation of intracellular cAMP or extracellular K^+ significantly enhanced aspects of hHCN1 currents. However, these manipulations did not significantly affect the capsazepine-induced inhibition of hHCN1.

6 The development of structural analogues of capsazepine may yield compounds that could selectively inhibit HCN channels and prove useful for the treatment of neurological disorders where a role for HCN channels has been described.

British Journal of Pharmacology (2004) **143,** 411–421. doi:10.1038/sj.bjp.0705945

Keywords: Recombinant HCN; human HCN1; I_h; capsazepine

Abbreviations: CHO, Chinese hamster ovary; DMEM, Dulbecco's modified Eagles medium; GFP, green fluorescent protein; h, human; HCN, hyperpolarization-activated cyclic nucleotide-gated; I_h, hyperpolarization-activated current $V_{1/2}$, half-maximal activation potential; VR1, vanilloid receptor 1; V_{rev}, reversal potential; ZD 7288, 4-ethyl-phenylamino-1,2-dimethyl-6-methylaminopyrimidinium chloride

Introduction

Hyperpolarization-activated cyclic nucleotide gated (HCN) ion channels are widely expressed on both neuronal and non-neuronal cells, where they fulfil numerous physiological roles. To date, four mammalian HCN subunits have been cloned (from human, rat, rabbit and mouse), which have been termed HCN 1–4 (Santoro *et al*., 1997; 1998; Ludwig *et al*., 1998; Seifert *et al*., 1999; reviewed by Kaupp & Seifert, 2001). The current mediated by these subunits (whether expressed alone, in different heteroligomeric combinations or natively) is most often referred to as I_h. Classically, this current plays an important pacemaker role in controlling cellular excitability. For example, in thalamic circuits I_h regulates the periodicity of network oscillations generated by thalamic relay neurones (Luthi & McCormick, 1998; Luthi *et al*., 1998). Nonpacemaking roles have also been described and include (a) a contribution to neuronal resting membrane potentials, (b) presynaptic modulation of neurotransmitter release (Pape, 1996; Beaumont & Zucker, 2000; Southan *et al*., 2000) and (c) modulation of the dendritic integration of inhibitory and excitatory synaptic inputs (Schwindt & Crill, 1997; Magee, 1998; 1999).

Given these wide-ranging roles of I_h, it is not surprising that HCN channels have been implicated in a number of disease processes. Most recently, a role in nociceptive processing has been proposed, based on the observation that repetitive activation of C fibres causes a post firing hyperpolarization that is enhanced by the inhibition of I_h. This has the overall effect of reducing the probability of further action potential generation and restricts information transfer through

*Author for correspondence; E-mail: Ceri_2_Davies@gsk.com
Advance online publication: 6 September 2004

peripheral axons (Dalle *et al*., 2001). As such, I_h can now be considered a potential target for the treatment of pain along with other ion-channels such as the vanilloid receptor VR1 (TRPV1). In this respect, it is interesting to note that HCN channels exhibit structural similarities to VR1 (see e.g. Gunthorpe *et al*., 2002; Robinson & Siegelbaum, 2003) and, although gated through different mechanisms, both ion channels operate as nonspecific cation channels. Furthermore, both VR1 and HCN channels are expressed in peripheral sensory neurones and their expression levels (VR1, HCN1 and HCN2) are significantly altered by neuropathic pain (Hudson *et al*., 2001; Chaplan *et al*., 2003). With respect to VR1, capsazepine has classically been used as the antagonist of choice to define the role of this receptor ($IC_{50} = 0.2$–$5.0\,\mu$M; e.g. Bevan *et al*., 1992; Liu & Simon, 1997) in a variety of preclinical pain models (*e.g*. Walker *et al*., 2003). However, it is now known that this compound also inhibits other cationic channels, for example, ligand-gated nicotinic acetylcholine receptors and voltage-dependent cationic channels (both calcium and potassium; Kuenzi & Dale, 1996; Docherty *et al*., 1997; Liu & Simon, 1997). Considering that HCN channels are voltage-activated and are implicated in pain processing, it is interesting that capsazepine exhibits certain structural features that are similar to those of the use-dependent I_h blocker zatebradine (VanBogaert *et al*., 1990; see Figure 2a). As a result of these observations, we were interested to examine whether or not capsazepine also affected I_h. To do this, we have examined how capsazepine affects currents generated by the homomeric assembly of human HCN1 (hHCN1) subunits.

Methods

Isolation of a clone for human HCN1

An assembly of human genomic sequence, plus a partial cDNA clone (AF064976), was compiled, predicting a 2670 nucleotide clone for full-length hHCN1 with an upstream stop codon. Mispriming due to the high GC content at the 5′ end of the gene made it difficult to amplify the full-length cDNA in a single reaction. To overcome the structural constraints, first-strand cDNA was generated from hypothalamus total RNA using HCN1 gene-specific primer (CAGTCCTAAAATTCAT GATCAGG) and the thermostable reverse transcriptase Thermoscript (Life Technologies) at 57°C. PCR using the GC-rich PCR system (Roche) (5′ AGGCGCGCAGCTAGC, 3′ TAGGAAAACTGTATCTGATGCC) was used to amplify the 5′ end fragment from the Thermoscript template. The 3′ 2.4 kb of the gene was amplified using PfuTurbo (Stratagene) to generate an overlapping fragment with the 5′ end (5′ CTCCGTGTGCTTCAAGG, 3′ AGGCTAGAGGGATC TATCAGG). Both 5′ and 3′ fragments were inserted into PCR 3.1 TOPO (Invitrogen), clones isolated and double-stranded sequenced. The full-length cDNA was assembled using a unique *Nco*I site (position 521 bp) present in the overlap between 5′ and 3′ fragments and inserted into pBluescript SK + (Stratagene) as a *Hind*III/*Xba*I fragment. The full-length clone was re-sequenced, as were independent clones for both the 5′ and 3′ fragments amplified from a hippocampus cDNA template.

For the transient transfection studies in CV-1 cells, the hHCN1 cDNA was excised out of pBluescript SK + as a *Hind*III/*Xba*I fragment and subcloned into the *Hind*III and *Xba*I sites in pcDNA3.1Hygro (In Vitrogen). For expression in Chinese hamster ovary (CHO) cells, the full-length sequence encoding hHCN1 was re-amplified using Pfu Turbo (Stratagene) to generate a consensus sequence for the initiation of translation (Kozak sequence) at the 5′ end (5′ GATCAGG TACCGCCACCATGGAAGGAGGCGGCAAGCCC 3′, 5′ GATCAGCGGCCGCTCATAAATTTGAAGCAAATCGTGG 3′). The full-length cDNA was subcloned into a mammalian expression vector pCIN5 (Rees *et al*., 1996) as a *Bam*HI/Blunt-end fragment. The full-length clone was re-sequenced.

Transient transfection of CV-1 cells

CV-1 cells were maintained in Dulbecco's modified Eagles medium (DMEM), 10% foetal bovine serum and 2 mM L-glutamine. The day before transfection, cells were plated onto 60 mm tissue culture dishes at a density of 8×10^5 cells per dish and incubated overnight at 37°C, 5% CO_2. Transient transfections were carried out with the hHCN1 plasmid and green fluorescent protein (GFP) using lipofectamine plus reagent. In brief, 1.5 μg hHCN1 DNA and 150 ng GFP were pre-complexed for 15 min at room temperature (RT). Pre-complexed DNA was added to 11.5 μl lipofectamine diluted in 290 μl DMEM and incubated for a further 15 min at RT. CV-1 cells were washed once with DMEM (no serum) and left in a volume of 2 ml of DMEM. Complexed DNA was added to the cells, gently mixed and incubated for 3 h at 37°C, 5% CO_2. Finally, 5 ml of growth media was added and the cells incubated overnight before being re-plated onto glass coverslips coated with 100 μg ml^{-1} poly-D-lysine at a density of 15,500 cells cm^{-2}.

Construction of stably expressing CHO cell line

CHO cells were maintained at 37°C with 5% CO_2 in a humidified incubator. Cells were grown in Iscove's modified Dulbecco's medium with L-glutamine (2 mM), supplemented with 10% foetal bovine serum, 100 μg ml^{-1} penicillin/streptomycin and 1 × nonessential amino acids. Stable transfection of CHO cells was carried out using lipofectamine 2000, according to the manufacturer's instructions. After incubating these cells for 48 h in nonselective medium, 0.8 mg ml^{-1} of G418 was added and the cells were grown for 3–4 weeks. G418-resistant clonal cell lines were obtained by limiting dilution cloning. These cell lines were screened for functional expression by electrophysiology. One of these cell lines was used in the biophysical analyses described here, and was maintained by propagation in medium containing 0.8 mg ml^{-1} of G418.

Electrophysiological recordings

Whole-cell patch-clamp recordings of hyperpolarization-activated membrane currents were performed at room temperature (18–21°C) using an Axoclamp 200B amplifier (Axon Instruments). The cells were continually superperfused at a rate of 3–5 ml min^{-1} with an extracellular solution comprising (in mM): 140 NaCl, 5 KCl, 2 $CaCl_2$, 1 $MgCl_2$, 10 D-glucose and 10 HEPES at pH 7.3. Patch electrodes were constructed from borosilicate glass (Clark) and filled with a pipette solution

comprising (in mM): 135 K gluconate, 10 $MgCl_2$, 0.1 $CaCl_2$, 1 EGTA, 10 HEPES, pH 7.2. Using these solutions, electrode resistances were within the range of 3–5 MΩ. The liquid junction potential, calculated to be 16 mV, has been accounted for in the results presented. Series resistances were between 4 and 11 MΩ. Cells were routinely voltage-clamped at −56 mV (junction-potential corrected) unless stated otherwise, and voltage-step protocols were applied using pClamp8 software (Axon Instruments). In most recordings from the CHO cells stably expressing HCN-1, we additionally applied a P-over-4 leak subtraction protocol to isolate HCN-1-mediated currents from the background leak conductance. Some considerable care was taken to establish this protocol such that it did not induce artifacts. Specifically, leak subtraction pulses were applied after the test pulse, having allowed sufficient time for complete HCN current deactivation. The holding potential for the leak subtraction epochs was −61 mV and the pulses were depolarizing in direction. Both leak-subtracted and non-leak-subtracted data were stored on the PC and were systematically compared during analysis to guard against the introduction of leak-subtraction-generated errors.

Data analysis

All data were captured using pClamp8 or 9 software (Axon Instruments) and filtered at 5 kHz. Digitized records were stored on the hard disk of a PC for off-line analysis using Clampfit 8 or 9 software (Axon Instruments) and Origin (Microcal Software). Data are expressed as the mean ± standard error of the mean from 3–17 cells.

Current–voltage relationships were obtained by hyperpolarizing the cell to −166 mV (for 750 ms duration) and measuring the amplitude of the tail current resulting from a series of depolarizing steps, from −166 to +14 mV (in 20 mV increments). Tail currents were normalized to the maximum amplitude recorded in either control conditions or each data set and plotted as a function of membrane potential. Activation curves were constructed by bringing the membrane potential to values between −36 and −176 mV (in 10 mV increments and either 1 or 4 s duration) and measuring the amplitude of the tail current produced when the membrane potential was stepped to +24 mV. Currents were normalized to the maximum amplitude recorded in either control conditions or each data set and plotted as a function of the prepulse potential. The resultant activation curve was fitted to the Boltzmann function:

$$I/I_{max} = [1 + \exp((V - V_{0.5})/k)]^{-1}$$

where V is the membrane potential, $V_{0.5}$ the potential at which I_h is half maximally activated and k the slope factor. Time constants of hHCN1 activation and deactivation were determined by fitting with either a mono- or bi-exponential function.

Reagents

All cell culture reagents were obtained from Life Technologies, with the exception of poly-D-lysine (Sigma, U.K.) and lipofectamine (Invitrogen, U.K.). Drugs were dissolved in water or DMSO (<0.1% final concentration) and applied by addition to the perfusing extracellular solution, except for two sets of experiments in which capsazepine and cAMP were applied intracellularly *via* incorporation in the recording electrode solution. 4-Ethylphenylamino-1,2-dimethyl-6-methylaminopyrimidinium chloride (ZD 7288) and *N*-[2-(4-chlorophenyl)ethyl]-1,3,4,5-tetrahydro-7,8-dihydroxy-2*H*-2-benzazepine-2-carbothioamide (capsazepine) were obtained from Tocris Cookson, U.K. 1,3,4,5-tetrahydro-7,8-dimethoxy-3-[3-[[2-(3,4-dimethoxyphenyl)ethyl]methyl-imino]-propyl]-2*H*-3benzazepin-2-*on*-hydrochloride (zatebradine) was synthesized at GlaxoSmithKline, U.K. cAMP was purchased from Sigma.

Results

Basic properties of hHCN1 channels

Heterologous expression of hHCN1 cDNA, either transiently in CV-1 cells, or stably in CHO cells, resulted in the formation of functional homomeric ion channels, which displayed a slowly activating inward current, characteristic of native I_h, upon hyperpolarization of the cell membrane. hHCN1-mediated currents appeared kinetically complex, as previously reported by others (Altomare *et al*., 2001). The rate of current activation was increased as the extent of hyperpolarization within the test pulse was increased (see control data set in Figure 6 for an example). The current activation trajectory of a 750 ms hyperpolarization to −146 mV could be fit with either a single- or two-exponential function fit. For nine typical recordings, the best single-exponential fit to the hHCN1 current activation trajectory had a time constant of 155 ± 10 ms. Two exponential fits generated mean time constants of 49 ± 12 and 246 ± 42 ms, with the latter time constant accounting for 29.5 ± 9.1% (Figure 1a). Combining these values produced a weighted pseudo-single exponential activation time constant of 168 ± 15 ms, similar to the value obtained with a single-exponential fit. As such, in all subsequent analyses of activation kinetics single-exponential fits have been used.

The rate of current activation could be enhanced by either the introduction of intracellular cAMP (Figure 1b) or by applying a hyperpolarizing prepulse (Figure 1c). The latter effect arose from an increase in the contribution of the fast activation component to the total activation process (KH and AR, unpublished observations). No evidence for macroscopic inactivation was found even with test pulses of up to 60 s duration (Figure 1d). Indeed, such test pulses suggested the possible presence of an ultraslow component in the activation process. Deactivation was classically slow at potentials either side of the reversal potential, but was speeded by depolarization (see control data set in Figure 5 for an example). Furthermore, the deactivation kinetics were complex, typically exhibiting a sigmoidal trajectory as previously reported elsewhere for other HCN channels (Altomare *et al*., 2001).

Inhibition of hHCN1-mediated currents by Cs^+, ZD 7288 and zatebradine

The established I_h blockers Cs^+ (5 mM), ZD 7288 (100 μM) and zatebradine (10 μM) inhibited hHCN1-mediated currents by 99 ± 1% (n = 4), 98 ± 1% (n = 5) and 92 ± 4% (n = 3), respectively (Figure 2b). Consistent with previous reports on native I_h (BoSmith *et al*., 1993), ZD 7288 was an apparently non-use-dependent blocker of the hHCN1-mediated current (Figure 2c).

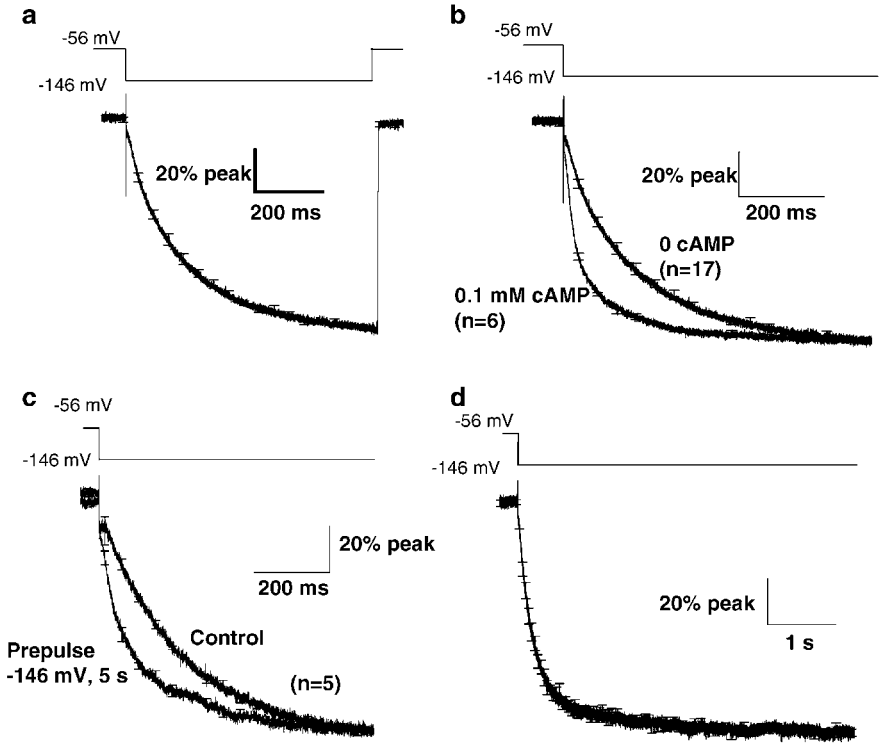

Figure 1 Basic gating properties of hHCN1-mediated currents. (a) A peak-normalized averaged hHCN1-mediated current from a CHO cell stably expressing hHCN1. Currents were elicited in 17 cells by hyperpolarizing the membrane from −56 to −146 mV for 750 ms (see the protocol shown), the current trace from each cell was normalized to the mean current amplitude observed during the last 20 ms of the test pulse, before being averaged across cells. Occasional error bars from the averaging process are shown. (b) A comparison of the activation kinetics of the hHCN1-mediated currents shown in (a) and six cells from the same culture in which cAMP (0.1 mM) was introduced to the cytoplasm from the patch pipette. Data were normalized and averaged as for (a). (c) Control hHCN1-mediated currents and currents observed in the same cells following a 5 s conditioning prepulse to −146 mV. The prepulse (which is not shown) was separated from the test pulse by 400 ms at −10 mV (sufficient time for >90% deactivation). Traces are from five cells and were processed as described for (a). (d) A peak-normalized average response to a 5 s hyperpolarization to −146 mV from a holding potential of −56 mV. Note the lack of macroscopic inactivation. Data were normalized and averaged as described for (a).

Thus, applying 10 μM ZD 7288 for 7 min, without activating hHCN1, initially resulted in a 33±2% inhibition of the inward current ($n=3$); a value similar to that observed when ZD 7288 (10 μM) was applied for 7 min and hHCN1 was activated every 20 s (30±3% inhibition; $n=4$). In contrast, zatebradine inhibited hHCN1 in an overt use-dependent manner (Figure 2c), as previously reported for I_h recorded from mouse dorsal root ganglion neurones (Raes *et al*., 1998). Thus, 10 μM zatebradine had no effect on the amplitude of the hHCN1-mediated current when applied in the absence of channel activation, but gradually reduced the response amplitude over a 15-min period once repetitive channel activation was resumed (0.05 Hz), resulting in a 92% inhibition ($n=3$).

Inhibition of hHCN1-mediated currents by capsazepine

Having established that the hHCN1 channel exhibited a pharmacological profile similar to that previously reported for both native as well as recombinant rodent HCN channels, we next examined whether the VR1 antagonist capsazepine (IC_{50} at VR1 ≈ 0.2–5 μM; Bevan *et al*., 1992) had any activity at this homomeric HCN channel. Application of capsazepine inhibited hHCN1-mediated currents (evoked by hyperpolarization of the cell membrane from −56 to −136 mV, for a 750 ms duration) in a reversible and concentration-dependent manner, with an IC_{50} value of 7.9±0.7 μM (Figure 3a; $n=3$–7), when current amplitude was measured at the end of the hyperpolarizing voltage step.

Interestingly, the slowing of the kinetics of activation of hHCN1-mediated currents was much greater than that afforded by the 'non-use-dependent' and equipotent blocker ZD 7288 (10 μM). Thus, exponential fits of the activation kinetics of I_h (evoked by stepping the membrane potential from −66 to −136 mV) revealed a τ value of 1270±143 ms ($n=5$) in the presence of capsazepine (10 μM) compared to 180±11 ms ($n=10$) in control. In contrast, a τ value of 259±26 ms ($n=6$) was determined for the I_h activation kinetics (evoked by stepping the membrane potential from −66 to −136 mV) in the presence of ZD 7288 (10 μM). Furthermore, the rate at which capsazepine-induced inhibition developed was much faster than that afforded by ZD 7288 at an equipotent concentration of 10 μM (Figure 3a).

The clear slowing of the activation kinetics of hHCN1 currents by capsazepine has an important consequence for its pharmacological profile, in that the degree to which current amplitude is reduced by this compound exhibits a time dependence. This is illustrated in Figure 3b where a control current and one recorded in the presence of 20 μM capsazepine

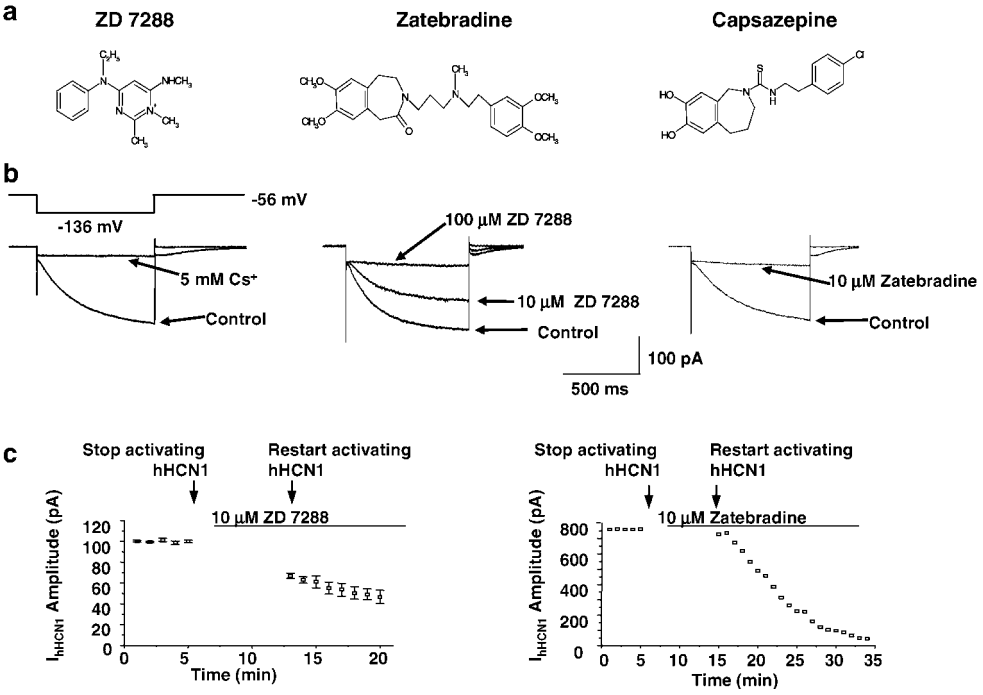

Figure 2 hHCN1 channels are inhibited by Cs^+, ZD 7288 and zatebradine. (a) Chemical structures of ZD 7288, zatebradine and capsazepine. (b) Hyperpolarization of the cell membrane potential, from −56 to −136 mV for a 750 ms duration, evokes slowly activating inward-current responses which were inhibited by the known I_h blockers Cs^+ (99% blockade at 5 mM), ZD 7288 (59 and 98% block at 10 and 100 μM, respectively) and zatebradine (92% block at 10 μM). (c) Graphical illustrations that blockade of the hHCN1-mediated current by ZD 7288 is non-use-dependent and that zatebradine is a use-dependent blocker of hHCN1. Applying 10 μM ZD 7288 for 7 min, without activating hHCN1, initially resulted in a 33±2% inhibition of the inward current, a value similar to that observed when ZD 7288 (10 μM) was applied for 7 min and hHCN1 was activated every 20 s (30±3% inhibition). The continued reduction of the hHCN1-mediated current in the presence of ZD 7288, after resuming channel activation, reflects the slow rate at which ZD 7288-induced inhibition of this current develops. Conversely, the application of 10 μM zatebradine in the absence of channel activation had no effect on the amplitude of the hHCN1-mediated current; however, it gradually reduced the response amplitude over a 15-min period once repetitive channel activation was resumed (0.05 Hz), resulting in a 92% inhibition.

are shown. Below this, a plot of the fractional inhibition is shown for the corresponding timepoints within the 750 ms test pulse. What is clear is that the ratio between the current in the drug and the control current increases as the test pulse proceeds. For example, in this experiment, the capsazepine-mediated block was around 75% after 50 ms into the hyperpolarizing test pulse but only 45% after 750 ms of hyperpolarization. This raises the question of whether capsazepine will produce any block in the steady state (i.e. when very long or permanent hyperpolarizations are used to activate hHCN1). In this respect, fitting exponential functions and extrapolating to infinite time suggested that steady-state block would be present, although with a lower IC_{50} than that reported in Figure 3a.

In addition to this analysis, we applied a more direct experimental method of testing whether capsazepine could produce a steady-state block of hHCN1 (Figure 3c). In particular, we activated hHCN1-mediated currents with a 30 s duration step from −56 to −146 mV. At 5 s into this hyperpolarization, we rapidly jumped into 100 μM capsazepine for 20 s (a high concentration was required because capsazepine block at lower concentrations is relatively slow). As can be seen in Figure 3c, capsazepine produced a clear block of inward current that began to reverse on its removal. In three cells undergoing this protocol, the mean time constant of capsazepine inhibition of inward current was 11.5±2.9 s.

Next we examined whether capsazepine was a use-dependent inhibitor of hHCN1. In all experiments, antagonism by capsazepine was not overtly use-dependent as a 7-min application of 10 μM capsazepine in the absence of hHCN1 activation inhibited the current to a similar extent (71±9% ($n=4$); Figure 4a cf. Figure 3a) to that when the channel was activated every 20 s throughout the capsazepine application (63±3% ($n=7$)).

In addition, we examined whether capsazepine was capable of blocking hHCN1 when applied intracellularly (Figure 4b). To do this, a high concentration of capsazepine (100 μM) was included in the standard whole-cell recording solution. In a considerable number of, but not all, cells tested, this treatment seemed to result in the activation of an unknown channel of seemingly large conductance that compromised the quality of the recordings. In recordings where the deleterious activity was not a problem, robust hHCN1 currents were observed up to 30 min following the establishment of the whole-cell configuration ($n=11$ cells lasting between 6 and 31 min). Furthermore, no time-dependent changes in hHCN1 activation kinetics were observed during these recordings and the activation kinetics and voltage dependence of the hHCN1 currents appeared normal (i.e. like drug naïve controls) even after 30 min of intracellular application of 100 μM capsazepine. In three cells filled with 100 μM capsazepine, a subsequent extracellular application of 20 μM capsazepine produced its

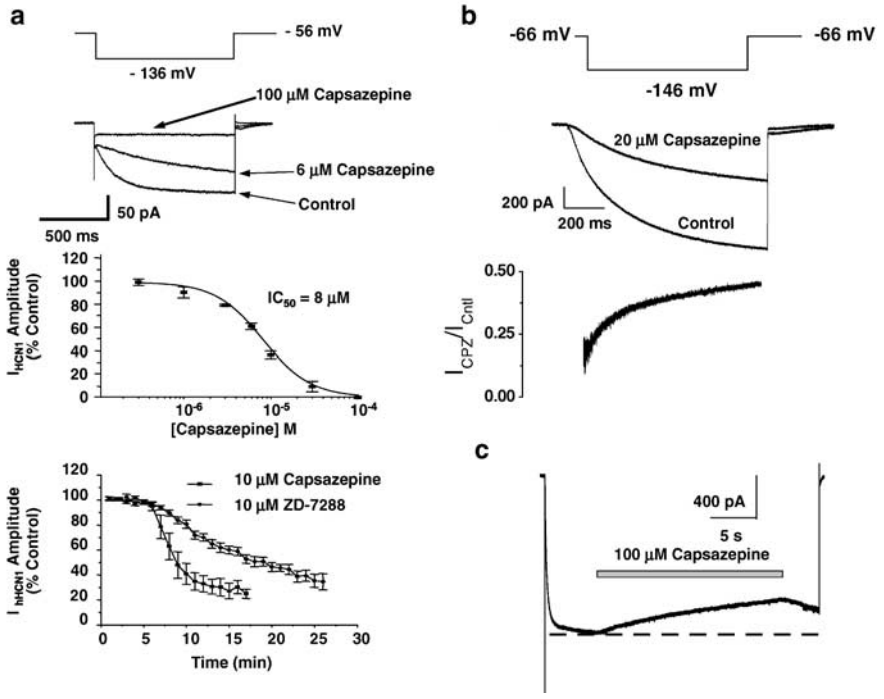

Figure 3 The vanilloid receptor antagonist capsazepine inhibits hHCN1 in a concentration- and time-dependent manner. (a) Application of capsazepine inhibited hHCN1-mediated currents (evoked by hyperpolarizing the cell membrane from −56 to −136 mV for 750 ms duration) in a reversible and concentration-dependent manner, with an IC_{50} value of 7.9 μM evaluated by measurement of the hHCN1-mediated current at the end of the hyperpolarizing step. The bottom graph illustrates that the rate at which the capsazepine-induced inhibition of the hHCN1 current developed much faster than that afforded by ZD 7288 at an 'equipotent' concentration (see Figure 2b middle traces) of 10 μM. (b) The uppermost trace illustrates a control current superimposed on one recorded in the presence of 20 μM capsazepine. Below these traces is a plot of the fractional inhibition induced by capsazepine throughout the timecourse of the 750 ms test pulse. Note that the ratio between the current in the drug and the control current increases as the test pulse proceeds. (c) illustrates a hHCN1-mediated current activated by a 30 s duration step from −56 to −146 mV. At 5 s into this hyperpolarizing step, 100 μM capsazepine was applied for 20 s. Note that capsazepine significantly inhibited the inward current, an effect that was reversed on its removal.

signature effects of a decrease in current amplitude (Figure 4b) and a 3.5±0.4-fold slowing of activation kinetics (activation time constant at –146 mV: control 121±23 ms *versus* 20 μM extracellular capsazepine 411±70 ms, $P<0.01$).

Voltage dependence of capsazepine-induced inhibition

Next we established whether the inhibition of hHCN1-induced currents was voltage-dependent. To do this, the current–voltage relationship of the hHCN1-mediated response was determined by fully activating the channel by hyperpolarizing cells to –166 mV and analysing the tail current amplitudes produced by depolarizing to + 14 mV, using a series of 20 mV steps (750 ms duration; Figure 5 ($n=4$)). The reversal potential (V_{rev}) for the current carried by hHCN1 was calculated to be −43±2 mV ($n=4$) and the inhibition of hHCN1 afforded by capsazepine (10 μM) was deemed to be voltage-independent (55±7% block at −166 mV ($n=4$) and 55±10% block at + 14 mV ($n=4$)) and not resulting from a change in V_{rev} (−43±3 mV; $n=4$, in the presence of 10 μM capsazepine).

It has been reported previously that inhibition of native I_h by either ZD 7288 or zatebradine is relieved by membrane hyperpolarization (Harris & Constanti, 1995; Raes *et al*., 1998). However, in several experiments, capsazepine-induced inhibition of hHCN1-mediated currents was not overtly reversed by prolonged (1 min) membrane hyperpolarization to −136 mV (not illustrated).

We also examined whether capsazepine affected the voltage-dependent activation profile of hHCN1. To determine the half-maximal activation potential ($V_{1/2}$) of hHCN1, a series of hyperpolarizing steps (in 10 mV increments and 1 s duration) to −176 mV were delivered. Terminating each step with a depolarizing pulse to + 24 mV produced a series of tail currents of graded amplitudes. A Boltzmann function fit of the peak amplitude of these currents yielded a $V_{1/2}$ value of −106±1 mV ($n=8$; Figures 6a and b). Since relatively short hyperpolarizing steps have been reported to result in an underestimation of the open probability of I_h tail current amplitudes, due to incomplete channel activation, which artificially shifts $V_{1/2}$ to more hyperpolarized values (Seifert *et al*., 1999), we investigated whether lengthening the duration of the hyperpolarizing pulses resulted in a shift of $V_{1/2}$. Prolonging the hyperpolarization step, from 1 to 4 s, shifted the half-maximal activation potential to −87±3 mV ($n=6$). Irrespective of the length of the hyperpolarizing step used, capsazepine (10 μM) induced a leftward shift in the hHCN1 activation curve. Thus, for 1 s hyperpolarizing steps, the $V_{1/2}$ in the presence of capsazepine was shifted by 34 mV to −140±2 mV ($n=4$) and for 4 s hyperpolarizing steps it was shifted by 33 mV to −120±2 mV ($n=5$).

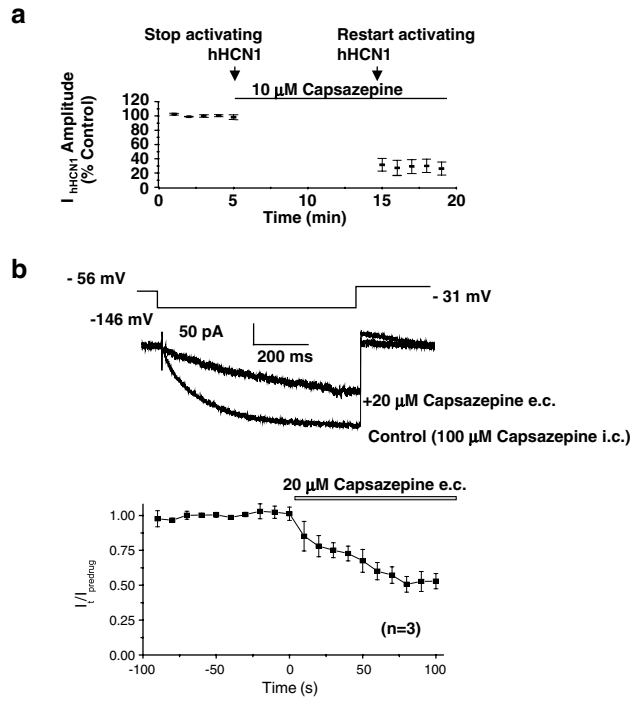

Figure 4 Capsazepine inhibits hHCN1-mediated currents in a non-use-dependent manner that does not require intracellular access to the ion channel. (a) illustrates the non-use-dependent inhibition of the hHCN1 current by capsazepine. Thus, application of 10 μM capsazepine in the absence of hHCN1 activation inhibited the current to a similar extent ($71 \pm 9\%$) to that when the channel was activated every 20 s throughout the capsazepine application ($63 \pm 3\%$). (b) The current traces are a control current recorded with 20 μM capsazepine within the whole-cell patch-clamp electrode solution superimposed on one recorded in the additional extracellular presence of 20 μM capsazepine. Below these traces is a plot of the fractional inhibition induced by extracellular capsazepine applied at time $t = 0$.

Previously, it has been reported that activation and deactivation kinetics for native I_h are voltage-dependent (Harris & Constanti, 1995; Magee, 1998). When the inward current responses mediated by activation of hHCN1 were fitted by a mono-exponential function (Figure 6e), the activation time constant (τ) in control conditions increased with membrane depolarization, from 158 ± 44 ms at -176 mV ($n = 5$) to 351 ± 46 ms at -116 mV ($n = 5$). In the presence of 10 μM capsazepine, τ was significantly enhanced at all test potentials investigated and ranged from 643 ± 45 ms ($n = 5$) at -176 mV to 1718 ± 190 ms ($n = 5$) at -116 mV. Conversely, the deactivation time constant (quantified by measuring the tail current decay time constant when stepping the membrane potential from -176 to $+24$ mV) was not observed to be significantly different between control responses (49 ± 7 ms; $n = 5$) and those recorded in the presence of 10 μM capsazepine (48 ± 8; $n = 5$; not illustrated).

Effect of capsazepine on pre-potentiated hHCN1 currents

Physiologically, HCN-mediated currents can be enhanced through modulation by, for example, elevations in intracellular cAMP or extracellular potassium concentration. To examine how these modifications affected the inhibitory effect of capsazepine, two experiments were performed.

In the first, intracellular cAMP levels were increased by including this cyclic nucleotide in the whole-cell recording solution. Although the mid-point voltage for activation of HCN1 channels is reported to only be slightly altered by cAMP when compared to other HCN channels, we found that inclusion of cAMP in the patch pipette, at 100 μM, considerably speeded hHCN1 current activation at -146 mV. Thus, in control cells the best-fit single exponential to the current activation trajectory had a mean time constant of 143 ± 14 ms, whereas in cAMP-filled cells the equivalent time constant was 51 ± 10 ms ($P < 0.00002$, unpaired t-test). Despite this alteration in activation kinetics, hHCN1 currents were still sensitive to inhibition by capsazepine (20 μM) when cells were filled with cAMP (Figure 7a).

In the second experiment, the effect of elevating extracellular K^+ on capsazepine-induced inhibition of hHCN1 currents was investigated. Elevation of the external K^+ concentration from 5 to 25 mM enhanced the hHCN1-mediated current (by $378 \pm 38\%$ ($n = 5$)) evoked in response to hyperpolarizing steps from -66 to -136 mV every 20 s, an effect mediated only in part through a depolarizing shift in I_h reversal potential. Despite this increase in I_h amplitude, the degree of inhibition induced by 10 μM capsazepine was unchanged, amounting to $67 \pm 5\%$ in 25 mM K^+ ($n = 5$) as opposed to $63 \pm 3\%$ in 5 mM K^+ ($n = 7$; Figure 7b).

Discussion

hHCN1 characteristics

In the present study, we have demonstrated that the human HCN1 subunit (hHCN1), when expressed in mammalian cell lines, forms functional recombinant hyperpolarization-activated ion channels with electrophysiological characteristics analogous to those of channels assembled from HCN1 subunits cloned from rodent species (Santoro *et al*., 2000; Shin *et al*., 2001). The pharmacological properties of the hHCN1 channel appear to be similar to those previously described for both native and recombinant HCN channels. Thus, ZD 7288 and zatebradine were effective inhibitors of hHCN1-mediated currents, exhibiting their characteristic apparent use- (zatebradine; Raes *et al*., 1998) and non-use- (ZD 7288; BoSmith *et al*., 1993; Harris and Constanti, 1995) dependent inhibitory signatures determined in whole-cell patch-clamp recordings (cf. Shin *et al*., 2001).

Capsazepine as an HCN channel blocker

We demonstrate further that capsazepine is capable of inhibiting hHCN1-mediated currents. The mechanism by which this occurs appears to be unrelated to a change in reversal potential of the hHCN1-mediated current and is both reversible, voltage- and use-independent, under whole-cell voltage-clamp conditions, thereby differing from the mechanism by which ZD 7288 and zatebradine have been reported to induce I_h inhibition (Harris & Constanti, 1995; Raes *et al*., 1998). Furthermore, capsazepine-induced block differs from ZD 7288-induced block with respect to the time course over which it develops, with the rate of

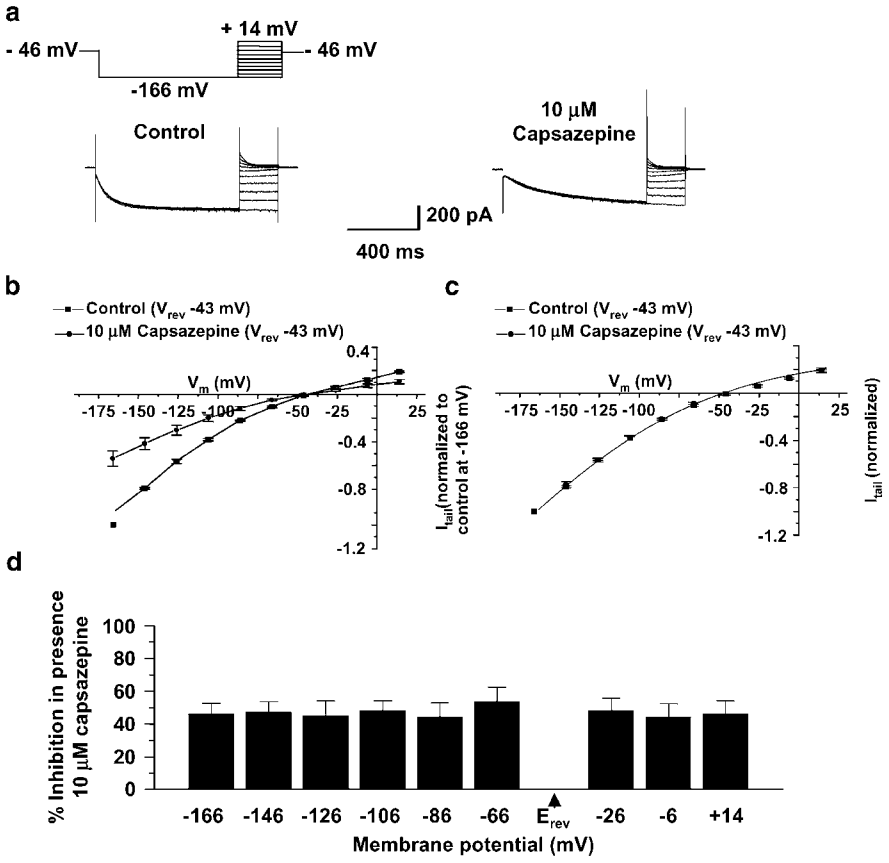

Figure 5 Blockade of hHCN1 by capsazepine is not voltage-dependent. (a) The current–voltage relationship of the hHCN1-mediated response was determined by fully activating the channel by hyperpolarizing cells to −166 mV and analysing the tail current amplitudes produced by depolarizing to +14 mV, using a series of 20 mV steps (750 ms duration). The voltage dependence of the capsazepine-induced inhibition of hHCN1 was determined by repeating this voltage protocol, following the induction of a steady-state partial inhibition by 10 μM capsazepine. (b) Graphical depiction of the current–voltage relationship. The data are normalized to the maximum tail current (recorded at −166 mV) in control conditions. The reversal potential (V_{rev}) for the current carried by hHCN1 was calculated to be −43±2 mV in control conditions and was unchanged in the presence of 10 μM capsazepine. (c) Same data set as in (b), however, normalized to the maximum tail current recorded in each data set. (d) Graph illustrating the percentage inhibition of the hHCN1-mediated current, induced by 10 μM capsazepine, at each of the test potentials investigated. Inhibition of hHCN1 afforded by capsazepine was voltage-independent with 55±7% block at −166 mV and 55±10% block at +14 mV.

capsazepine-induced block being 5× faster than that induced by ZD 7288. However, perhaps the most striking feature of the inhibition by capsazepine is the dramatic slowing of the kinetics of activation of hHCN1-mediated currents. Such an effect is also induced by ZD 7288, although this is only observed at holding potentials more depolarized than −110 mV. Even then the magnitude of this effect is up to 100× less than that observed with capsazepine in the present study (Harris & Constanti, 1995). As a result of this, the degree to which capsazepine reduces the hHCN1 current amplitude is highly time dependent, with the apparent IC_{50} value effectively increasing with increasing step duration. In this respect, the experiment illustrated in Figure 3 indicates that at steady state activation of hHCN-1 capsazepine exhibits an IC_{50} $\geqslant$100 μM. Although this appears to be a very weak antagonism, the substantial slowing of activation kinetics at much lower concentrations of capsazepine, and the more potent non-steady-state IC_{50} this produces, will result in significant effects on the physiology of hHCN1-expressing cells. Mechanistically, parallels can be drawn to the slowing of presynaptic calcium channel activation elicited by Gi/o-coupled G-protein-coupled receptors.

Hyperpolarizing shift in the voltage dependence of activation

Considering the voltage dependence of activation of hHCN1-mediated currents, it was apparent that capsazepine routinely caused a 30–40 mV hyperpolarizing shift in the voltage for half-maximal activation of I_h, an effect that would account, at least in part, for the inhibition afforded by this molecule. However, this effect may also arise from the slowing of the kinetics of activation of hHCN1-mediated currents. To understand this, we must first consider the voltage dependence of activation of hHCN1-mediated currents. Specifically, in control medium, the rate of activation of hHCN1-mediated currents becomes much faster as the holding potential is hyperpolarized. In the presence of capsazepine, the rate of activation is dramatically slowed at all holding potentials although the trend for increased activation rates with

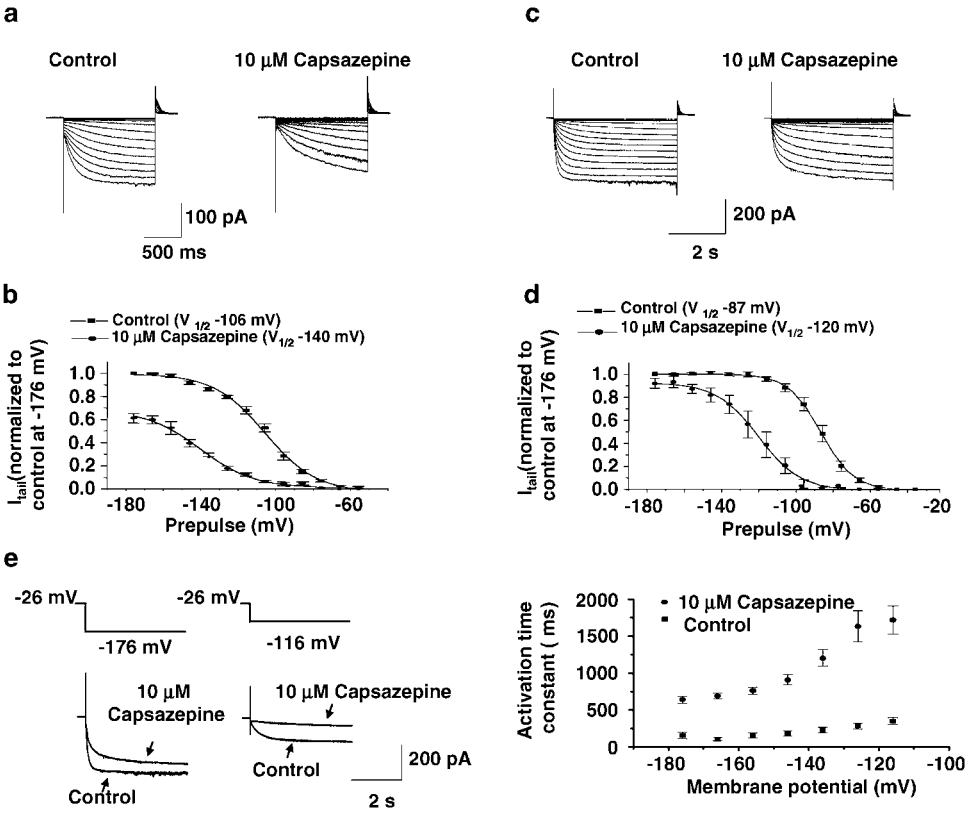

Figure 6 Blockade of hHCN1 by capsazepine results in a leftward shift of the activation curve and a slowing of current activation kinetics. (a) The half-maximal activation potential ($V_{1/2}$) of hHCN1 was determined by delivering a series of hyperpolarizing steps (in 10 mV increments and 1 s duration) to −176 mV. Terminating each step with a depolarizing pulse to +24 mV produced a series of tail currents of graded amplitudes. This voltage protocol was repeated once a steady-state partial inhibition of the hHCN1-mediated response was achieved following the application of 10 μM capsazepine. (b) Graphical illustration of the hHCN1 activation curve determined in control and 10 μM capsazepine. The data are normalized to the maximum tail current (recorded by stepping from −176 to +24 mV) in control conditions. A Boltzmann function fit of the data yielded a $V_{1/2}$ value of −106±1 mV in control and −140±2 mV in 10 μM capsazepine. (c) As relatively short hyperpolarizing steps have been reported to result in an underestimation of the open probability of I_h tail current amplitudes, we also determined the hHCN1 activation curve by delivering the same series of hyperpolarizing steps, in 10 mV increments to −176 mV, and 4 s in duration. (d) Graphical illustration of the hHCN1 activation curve determined in control (■) and 10 μM capsazepine (●). The data are normalized to the maximum tail current (recorded at −176 mV) in control conditions. A Boltzmann function fit of the data yielded a $V_{1/2}$ value of −87±3 mV in control and −120±2 mV in 10 μM capsazepine. Irrespective of the length of the hyperpolarizing step capsazepine (10 μM) induced a 33–34 mV leftward shift in the hHCN1 activation curve. (e) Inward current responses mediated by the activation of hHCN1 were fitted by a mono-exponential function and the activation time constants (τ) were plotted against membrane potential in control conditions (■) and in the presence of 10 μM capsazepine (●). τ increased with membrane depolarization, from 158±44 ms at −176 mV to 351±46 ms at −116 mV in control conditions. In the presence of 10 μM capsazepine, τ was significantly enhanced at all test potentials investigated and varied from 643±45 ms at −176 mV to 1718±190 ms at −116 mV.

increasing hyperpolarization still applies. This slowing of activation rates can have a marked bearing on the apparent voltage dependence of activation of hHCN1-mediated currents because tail current analysis performed at a time point at which currents are submaximally activated will generate an artificially hyperpolarized $V_{1/2}$ for activation. For example, in control medium, suboptimal activation of HCN1 using 1 s long hyperpolarizing steps generates a $V_{1/2}$ of −110 mV as opposed to −80 mV when full activation of hHCN1-mediated currents is allowed by employing 4 s long voltage steps. Thus, slowing the kinetics of activation can easily account for the apparent 30–40 mV hyperpolarizing shift in $V_{1/2}$ observed in the presence of capsazepine. Indeed, it is no coincidence that a 4 s long step in the presence of capsazepine achieves a similar level of hHCN1-mediated current activation as a 1 s long step in control medium and that $V_{1/2}$ under these two conditions is (a) close to −120 mV and (b) some 30 mV hyperpolarized to the $V_{1/2}$ generated in control medium when 4 s long hyperpolarizing steps are employed. What is particularly striking in Figure 6 is that when cells are stepped to potentials more hyperpolarized than −130 mV for 4 s, capsazepine-induced inhibition of hHCN1-mediated currents is greatly reduced. The reason for this is that at these holding potentials the time constants of activation of hHCN1 channels in the presence and absence of capsazepine converge towards one another and the step time is sufficiently long to enable maximal activation of I_h.

Recombinant HCN channels display distinct activation kinetics. Thus, homomeric HCN1 activates more rapidly than homomeric HCN2 and both of these channels display faster activation kinetics than homomeric HCN4. The structural determinants responsible for such differences in activation kinetics have been investigated in chimeric channels constructed from HCN1 and HCN4 subunits (Ishii *et al.*, 2001). Two regions have been identified which contribute to

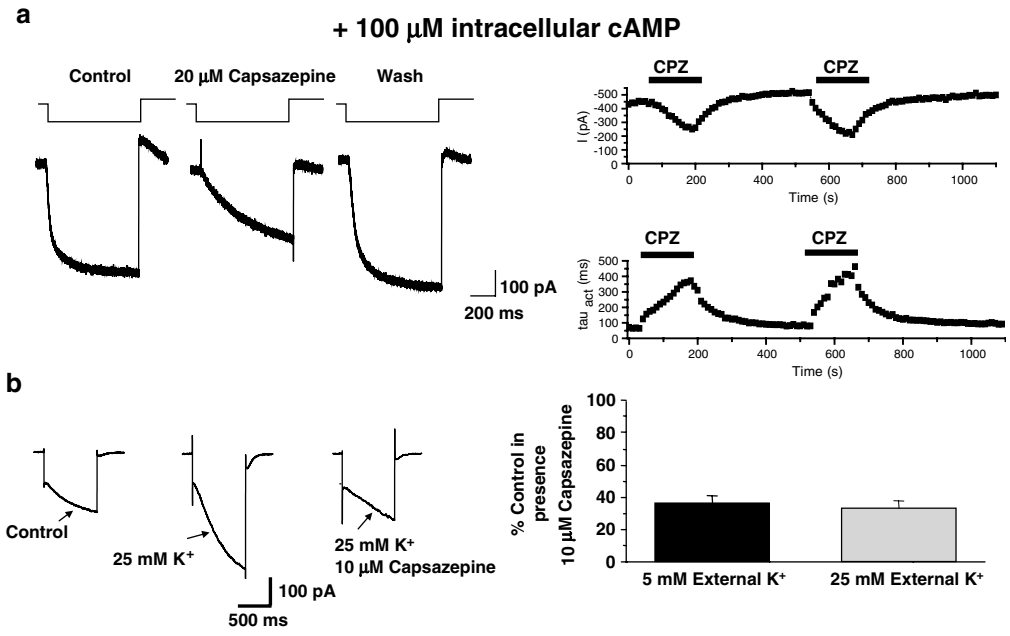

Figure 7 Potentiation of hHCN1-mediated currents through elevation of intracellular cAMP or extracellular K^+ does not significantly impair the inhibitory effect of capsazepine. (a) Traces from left to right are hHCN1 mediated currents recorded in the presence of 100 μM cAMP, in the additional presence of 20 μM capsazepine and following washout of this antagonist. The plots to the right illustrate the effects of two consecutive applications of capsazepine on peak current amplitude and time constant of activation. (b) Elevation of external [K^+] enhances the amplitude of I_{hHCN1} but has no effect on the magnitude of capsazepine antagonism. Elevation of the external K^+ concentration, from 5 to 25 mM, enhanced the hHCN1-mediated current (by 378$\pm$38%) evoked in response to hyperpolarizing steps from -66 to -136 mV, every 20 s. The degree of inhibition induced by 10 μM capsazepine was unchanged when the external [K^+] was raised i.e. 63$\pm$3% inhibition in 5 mM K^+, as opposed to 67$\pm$5% inhibition in 25 mM K^+.

activation kinetics: eight amino acids located in both the first transmembrane domain (S1) and the extracellular linking region between transmembrane domains S1 and S2, and also a smaller contribution from an intracellular domain located between transmembrane domain S6 and the cyclic nucleotide-binding domain. It would therefore be tempting to speculate that the slowing of the activation kinetics of hHCN1, by capsazepine, may in part be due to an interaction with this extracellular domain between S1 and S2, an observation supported by the finding that accelerating activation kinetics by raising intracellular cAMP did not appear to affect the ability of capsazepine to inhibit hHCN1. Additionally, given the very slow activation kinetics of HCN4, it would be of interest to determine the effect, if any, of capsazepine on the activation kinetics of homomeric HCN4 channels. Without access to these recombinant channels, we could not perform these experiments. However, it is noteworthy that capsazepine was capable of inhibiting I_h with different kinetic properties in hippocampal and DRG neurones.

Concluding remarks

While we have not addressed in detail the specific biophysical characteristics that account for the differences by which ZD 7288 and capsazepine block hHCN1, it is likely they reflect differences in the way in which ZD 7288 and capsazepine bind to HCN channels. In this respect, molecular modification of hHCN1 may provide a useful insight into the different binding sites occupied by distinct modulators of HCN channel function. This aside, the potential to synthesize ligands that exhibit different interactions with a given HCN isoform provides hope that we can develop molecules that selectively interact with distinct HCN isoforms. To date, no such pharmacological agents exist with all I_h blockers (including capsazepine (preliminary observations)), exhibiting activity at native channels from a variety of neuronal and non-neuronal preparations. However, all of these compounds exert other nonspecific effects that complicate interpretation of the role of I_h in synaptically coupled neuronal circuits (Chevaleyre & Castillo, 2002). As such, there is still a need for pharmacological tools that are devoid of other activities to unequivocally define the role of I_h in synaptic networks. Until this is achieved, care should be taken in using a single I_h blocker to define HCN channels as a mediator of particular physiological roles. Conversely, the use of capsazepine to define a physiological role as being mediated by activation of VR1 should be viewed as circumspect unless tested alongside other more specific VR1 antagonists, for example, iodo-resiniferatoxin and SB-366791 (Wahl *et al*., 2001; Gunthorpe *et al*., 2004), which does not affect I_h. Indeed, it is noteworthy that HCN channels have recently been implicated in nociceptive processing (Chaplan *et al*., 2003). Nevertheless, capsazepine does provide a starting molecule from which to develop future pharmacological agents that modify the activity of HCN channels in a manner different from existing inhibitors of I_h. Conceptually, different state-dependent inhibitors of I_h may ultimately be tailored specifically to interact with different physiological processes. As such, these compounds may have utility in the treatment of different disease states for which a role of I_h has been described.

References

ALTOMARE, C., BUCCHI, A., CAMATINI, E., BARUSCOTTI, M., VISCOMI, C., MORONI, A. & DIFRANCESCO, D. (2001). Integrated allosteric model of voltage-gating of HCN channels. *J. Gen. Physiol.,* **117,** 519–532.

BEAUMONT, V. & ZUCKER, R.S. (2000). Enhancement of synaptic transmission by cyclic AMP modulation of presynaptic I_h channels. *Nature,* **3,** 133–141.

BEVAN, S., HOTHI, S., HUGHES, G., JAMES, I.F., RANG, H.P., SHAH, K., WALPOLE, C.S. & YEATS, J.C. (1992). Capsazepine: a competitive antagonist of the sensory neurone excitant capsaicin. *Br. J. Pharmacol.,* **107,** 544–552.

BOSMITH, R.E., BRIGGS, I. & STURGESS, N.C. (1993). Inhibitory actions of ZENECA ZD 7288 on whole-cell hyperpolarization activated inward current (I_f) in guinea-pig dissociated sinoatrial node cells. *Br. J. Pharmacol.,* **110,** 343–349.

CHAPLAN, S.R., GUO, H.Q., LEE, D.H., LUO, L., LIU, C., KUEI, C., VELUMIAN, A.A., BUTLER, M.P., BROWN, S.M. & DUBIN, A.E. (2003). Neuronal hyperpolarization-activated pacemaker channels drive neuropathic pain. *J. Neurosci.,* **23,** 1169–1178.

CHEVALEYRE, V. & CASTILLO, P.E. (2002). Assessing the role of I_h channels in synaptic transmission and mossy fibre LTP. *Proc. Natl. Acad. Sci. U.S.A.,* **99,** 9538–9543.

DALLE, C., SCHNEIDER, M., CLERGUE, F., BRETTON, C. & JIROUNEK, P. (2001). Inhibition of the I_h current in isolated peripheral nerve: a novel model of peripheral antinociception? *Muscle Nerve,* **24,** 254–261.

DOCHERTY, R.J., YEATS, J.C. & PIPER, A.S. (1997). Capsazepine block of voltage-activated calcium channels in adult rat dorsal root ganglion neurones in culture. *Br. J. Pharmacol.,* **121,** 1461–1467.

GUNTHORPE, M.J., BENHAM, C.D., RANDALL, A. & DAVIS, J.B. (2002). The diversity in the vanilloid (TRPV) receptor family of ion channels. *TIPS,* **23,** 183–191.

GUNTHORPE, M.J., RAMI, H.K., JERMAN, J., SMART, D., GILL, C.H., SOFFIN, E.M., LUIS HANNAN, S., LAPPIN, S.C., EGERTON, J., SMITH, G.D., WORBY, A., HOWETT, L., OWEN, D., NASIR, S., DAVIES, C.H., THOMPSON, M., WYMAN, P.A., RANDALL, A.D. & DAVIS, J.B. (2004). Identification and characterisation of SB-366791, a potent and selective vanilloid receptor (VR1/TRPV1) antagonist. *Neuropharmacology,* **46,** 133–149.

HARRIS, N.C. & CONSTANTI, A. (1995). Mechanism of block by ZD 7288 of the hyperpolarization-activated inward rectifying current in guinea-pig substantia nigra neurons *in vitro*. *J. Neurophysiol.,* **74,** 2366–2378.

HUDSON, L.J., BEVAN, S., WOTHERSPOON, G., GENTRY, C., FOX, A. & WINTER, J. (2001). VR1 protein expression increases in undamaged DRG neurons after partial nerve injury. *Eur. J. Neurosci.,* **13,** 2105–2114.

ISHII, T.M., TAKANO, M. & OHMORI, H. (2001). Determinants of activation kinetics in mammalian hyperpolarization-activated cation channels. *J. Physiol.,* **537,** 93–100.

KAUPP, U.B. & SEIFERT, R. (2001). Molecular diversity of pacemaker ion channels. *Annu. Rev. Physiol.,* **63,** 235–257.

KUENZI, F.M. & DALE, N. (1996). Effect of capsaicin and analogues on potassium and calcium currents and vanilloid receptors in *Xenopus* embryo spinal neurones. *Br. J. Pharmacol.,* **119,** 81–90.

LIU, L. & SIMON, S.A. (1997). Capsazepine, a vanilloid receptor antagonist, inhibits nicotinic acetylcholine receptors in rat trigeminal ganglia. *Neurosci. Lett.,* **228,** 29–32.

LUDWIG, A., ZONG, X., JEGLITSCH, M., HOFMANN, F. & BIEL, M. (1998). A family of hyperpolarization-activated mammalian cation channels. *Nature,* **393,** 587–591.

LUTHI, A., BAL, T. & MCCORMICK, D.A. (1998). Periodicity of thalamic spindle waves is abolished by ZD 7288, a blocker of I_h. *J. Neuophysiol.,* **79,** 3284–3289.

LUTHI, A. & MCCORMICK, D.A. (1998). Periodicity of thalamic synchronized oscillations: the role of Ca^{2+}-mediated upregulation of I_h. *Neuron,* **20,** 553–563.

MAGEE, J.C. (1998). Dendritic hyperpolarization-activated currents modify the integrative properties of hippocampal CA1 pyramidal neurons. *J. Neurosci.,* **18,** 7613–7624.

MAGEE, J.C. (1999). Dendritic I_h normalizes temporal summation in hippocampal CA1 neurones. *Nat. Neurosci.,* **2,** 508–514.

PAPE, H.C. (1996). Queer current and pacemaker: the hyperpolarization-activated cation current in neurons. *Annu. Rev. Physiol.,* **58,** 299–327.

RAES, A., VAN DE VIJVER, G., GOETHALS, M. & VAN BOGAERT, P.P. (1998). Use-dependent block of I_h in mouse dorsal root ganglion neurons by sinus node inhibitors. *Br. J. Pharmacol.,* **125,** 741–750.

REES, S., COOTE, J., STABLES, J., GOODSON, S., HARRIS, S. & LEE, M.G. (1996). Bicistronic vector for the creation of stable mammalian cell lines that predisposes all antibiotic-resistant cells to express recombinant protein. *Biotechniques,* **20,** 102–104, 106, 108–110.

ROBINSON, R.B. & SIEGELBAUM, S.A. (2003). Hyperpolarization-activated cation currents: from molecules to physiological function. *Annu. Rev. Physiol.,* **65,** 453–480.

SANTORO, B., CHEN, S., LUTHI, A., PAVLIDIS, P., SHUMYATSKY, G.P., TIBBS, G.R. & SIEGELBAUM, S.A. (2000). Molecular and functional heterogeneity of hyperpolarization-activated pacemaker channels in the mouse CNS. *J. Neurosci.,* **20,** 5264–5275.

SANTORO, B., GRANT, S.G.N., BARTSCH, D. & KANDEL, E.R. (1997). Interactive cloning with the SH3 domain of N-src identifies a new brain specific ion channel protein, with homology to Eag and cyclic nucleotide-gated channels. *Proc. Natl. Acad. Sci. U.S.A.,* **94,** 14815–14820.

SANTORO, B., LIU, D.T., YAO, H., BARTSCH, D., KANDEL, E.R., SIEGLEBAUM, S.A. & TIBBS, G.R. (1998). Identification of a gene encoding a hyperpolarization-activated pacemaker channel of brain. *Cell,* **93,** 717–729.

SCHWINDT, P.C. & CRILL, W.E. (1997). Modification of current transmitted from apical dendrite to soma by blockade of voltage- and Ca^{2+}-dependent conductances in rat neocortical pyramidal neurons. *J. Neurophysiol.,* **78,** 187–198.

SEIFERT, R., SCHOLTEN, A., GAUSS, R., MINCHEVA, A., LICHTER, P. & KAUPP, U.B. (1999). Molecular characterization of a slowly gating human hyperpolarization-activated channel predominantly expressed in thalamus, heart and testis. *Proc. Natl. Acad. Sci. U.S.A.,* **96,** 9391–9396.

SHIN, K.S., ROTHBERG, B.S. & YELLEN, G. (2001). Blocker state dependence and trapping in hyperpolarization-activated cation channels: evidence for an intracellular activation gate. *J. Gen. Physiol.,* **117,** 91–101.

SOUTHAN, A.P., MORRIS, N.P., STEPHENS, G.J. & ROBERTSON, B. (2000). Hyperpolarization-activated currents in presynaptic terminals of mouse cerebellar basket cells. *J. Physiol.,* **526,** 91–97.

VANBOGAERT, P.P., GOETHALS, M. & SIMOENS, C. (1990). Use- and frequency-dependent blockade by UL-FS 49 of the pacemaker current in cardiac Purkinje fibres. *Eur. J. Pharmacol.,* **187,** 241–256.

WAHL, P., FOGED, C., TULLIN, S. & THOMSEN, C. (2001). Iodoresiniferatoxin, a new potent vanilloid receptor antagonist. *Mol. Pharmacol.,* **59,** 9–15.

WALKER, K.M., URBAN, L., MEDHURST, S.J., PATEL, S., FOX, A.J. & MCINTYRE, P. (2003). The VR1 antagonist capsazepine reverses mechanical hyperalgesia in models of inflammatory and neuropathic pain. *J. Pharmacol. Exp. Ther.,* **304,** 56–62.

(Received November 26, 2003
Revised May 13, 2004
Accepted July 8, 2004)